Galactic cosmic rays and gamma rays: a unified approach*

Andrew W. Strong[1] and Igor V. Moskalenko[1,2]
[1]Max-Planck-Institut für extraterrestrische Physik, Postfach 1603, D-85740 Garching, Germany
[2]Institute for Nuclear Physics, M.V.Lomonosov Moscow State University, 119 899 Moscow, Russia

ABSTRACT

We are constructing a model which aims to reproduce observational data of many kinds related to cosmic-ray origin and propagation: direct measurements of nuclei, antiprotons, electrons and positrons, γ-rays, and synchrotron radiation. These data provide many independent constraints on any model. Propagation of primary and secondary nucleons, primary and secondary electrons and positrons are calculated self-consistently. Fragmentation and energy losses are computed using realistic distributions for the interstellar gas and radiation fields, and diffusive reacceleration is also incorporated. The models are adjusted to agree with the observed cosmic-ray B/C and ^{10}Be/ ^{9}Be ratios.

Our main results include evaluation of diffusion/convection and reacceleration models, estimates of the halo size, calculations of the interstellar positron and antiproton spectra, evaluation of alternative hypotheses of hard nucleon and hard electron interstellar spectra, and computation of the Galactic diffuse γ-ray emission.

1. Introduction

We have developed a model which aims to reproduce self-consistently observational data of many kinds related to cosmic-ray origin and propagation: direct measurements of nuclei, antiprotons, electrons and positrons, γ-rays, and synchrotron radiation. These data provide many independent constraints on any model and our approach is able to take advantage of this since it must be consistent with all types of observation.

A numerical method and corresponding computer code (GALPROP) for the calculation of Galactic cosmic-ray propagation in 3D has been developed. The basic spatial propagation mechanisms are (momentum-dependent) diffusion and convection, while in momentum space energy loss and diffusive reacceleration are treated. Fragmentation and energy losses are computed using realistic distributions for the interstellar gas and radiation fields. The code is sufficiently flexible that it can be extended to include new aspects as required. The basic procedure is first to obtain a set of propagation parameters which reproduce the cosmic ray B/C and ^{10}Be/ ^{9}Be

* *Contribution to a book "Topics in Cosmic Ray Astrophysics", ed. M.A.DuVernois (NY: Nova Scientific), 1999*

ratios; the same propagation conditions are then applied to primary electrons. Gamma-ray and synchrotron emission are then evaluated with the same model.

Our approach is not intended to perform detailed source abundance calculations with a large network of reactions, which is still best done with the path-length distribution approach (see e.g. DuVernois, Simpson, & Thayer 1996 and references therein). Instead we use just the principal progenitors and weighted cross sections based on the observed cosmic-ray abundances (see Webber, Lee, & Gupta 1992). The B/C data is used since it is the most accurately measured ratio covering a wide energy range and having well established cross sections. A re-evaluation of the halo size is desirable since new ^{10}Be/ ^{9}Be data are available from Ulysses with better statistics than previously.

Preliminary results were presented in Strong & Moskalenko (1997) (hereafter Paper I) and full results for protons, Helium, positrons, and electrons in Moskalenko & Strong (1998a) (hereafter Paper II). Evaluation of the B/C and ^{10}Be/ ^{9}Be ratios, evaluation of diffusion/convection and reacceleration models, and setting of limits on the halo size, as well as full details of the numerical method and energy losses for nucleons and electrons are summarized in Strong & Moskalenko (1998) (hereafter Paper III). Evaluation of antiprotrons in connection with diffuse Galactic γ-rays and interstellar nucleon spectrum are given in Moskalenko, Strong, & Reimer (1998) (hereafter Paper IV). For a recent discussion of diffuse Galactic continuum γ-rays and synchrotron emission in the context of this approach see Strong, Moskalenko, & Reimer (1998) (hereafter Paper V) and Moskalenko & Strong (1998d).

For interested users our model is available in the public domain on the World Wide Web (*http://www.gamma.mpe-garching.mpg.de/∼aws/aws.html*)

2. Motivation

It was pointed out many years ago (see Ginzburg, Khazan, & Ptuskin 1980, Berezinskii et al. 1990) that the interpretation of radioactive cosmic-ray nuclei is model-dependent and in particular that halo models lead to a quite different physical picture from homogeneous models. The latter show simply a rather lower average matter density than the local Galactic hydrogen (e.g., Simpson & Garcia-Munoz 1988, Lukasiak et al. 1994a), but do not lead to a meaningful estimate of the size of the confinement region, and the correponding cosmic-ray 'lifetime' is model-dependent. In such treatments the lifetime is combined with the grammage to yield an 'average density'. For example Lukasiak et al. (1994a) find an 'average density' of 0.28 cm^{-3} compared to the local interstellar value of about 1 cm^{-3}, indicating a z-extent of less than 1 kpc compared to the several kpc found in diffusive halo models. Our model includes spatial dimensions as a basic element, and so these issues are automatically addressed.

The possible rôle of convection was shown by Jokipii (1976), and Jones (1979) pointed out its effect on the energy-dependence of the secondary/primary ratio. Recent papers give estimates for

the halo size and limits on convection based on existing calculations (e.g., Webber, Lee, & Gupta 1992, Webber & Soutoul 1998), and we attempt to improve on these models with a more detailed treatment.

Previous approaches to the spatial nucleon propagation problem have been mainly analytical: Jones (1979), Freedman et al. (1980), Berezinskii et al. (1990), Webber, Lee, & Gupta (1992), Bloemen et al. (1993), and Ptuskin & Soutoul (1998) treated diffusion/convection models in this way. Bloemen et al. (1993) used the 'grammage' formulation rather than the explicit isotope ratios, and their propagation equation implicitly assumes identical distributions of primary and secondary source functions. These papers did not attempt to fit the low-energy (< 1 GeV/nucleon) B/C data (which we will show leads to problems) and also did not consider reacceleration. It is clear than an analytical treatment quickly becomes limited as soon as more realistic models are desired, and this is the main justification for the numerical approach. The case of electrons and positrons is even more intractable analytically, although fairly general cases have been treated (Lerche & Schlickeiser 1982). Recently Porter & Protheroe (1997) made use of a Monte-Carlo method for electrons, with propagation in the z-direction only. This method would be very time-consuming for 2- or 3-D cases. Our method, using numerical solution of the propagation equation, is a practical alternative.

Reacceleration has previously been handled using leaky-box calculations (Letaw, Silberberg, & Tsao 1993, Seo & Ptuskin 1994, Heinbach & Simon 1995); this has the advantage of allowing a full reaction network to be used (far beyond what is possible in the present approach), but suffers from the usual limitations of leaky-box models, especially concerning radioactive nuclei, which were not included in these treatments. Our simplified reaction network is necessary because of the added spatial dimensions, but we believe it is fully sufficient for our purpose, since we are not attempting to derive a comprehensive isotopic composition. A more complex reaction scheme would not change our conclusions.

3. Description of the models

The models are three dimensional with cylindrical symmetry in the Galaxy, and the basic coordinates are (R, z, p), where R is Galactocentric radius, z is the distance from the Galactic plane, and p is the total particle momentum. The distance from the Sun to the Galactic centre is taken as $R_\odot = 8.5$ kpc. In the models the propagation region is bounded by $R = R_h$, $z = \pm z_h$ beyond which free escape is assumed. We take $R_h = 30$ kpc. The range $z_h = 1 - 20$ kpc is considered. For a given z_h the diffusion coefficient as a function of momentum is determined by B/C for the case of no reacceleration; if reacceleration is assumed then the reacceleration strength (related to the Alfvén speed) is constrained by the energy-dependence of B/C. The spatial diffusion coefficient for the case of no reacceleration is taken as $D_{xx} = \beta D_0 (\rho/\rho_0)^{\delta_1}$ below rigidity ρ_0, $\beta D_0 (\rho/\rho_0)^{\delta_2}$ above rigidity ρ_0, where the factor β $(= v/c)$ is a natural consequence of a random-walk process. Since the introduction of a sharp break in D_{xx} is a contrived procedure

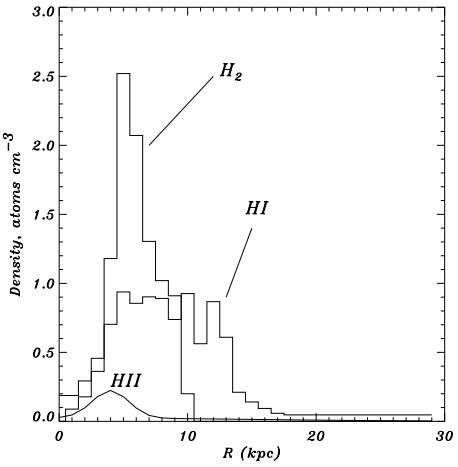

Fig. 1.— The adopted radial distribution of atomic (HI), molecular (H_2) and ionized (HII) hydrogen at $z = 0$.

which is adopted just to fit B/C at all energies, we also consider the case $\delta_1 = \delta_2$, i.e. no break, in order to investigate the possibility of reproducing the data in a physically simpler way. The convection velocity (in z-direction only) $V(z)$ is assumed to increase linearly with distance from the plane ($V > 0$ for $z > 0$, $V < 0$ for $z < 0$, and $dV/dz > 0$ for all z); this implies a constant adiabatic energy loss. The linear form for $V(z)$ is suggested by cosmic-ray driven MHD wind models (e.g., Zirakashvili et al. 1996).

We include diffusive reacceleration since some stochastic reacceleration is inevitable, and it provides a natural mechanism to reproduce the energy dependence of the B/C ratio without an *ad hoc* form for the diffusion coefficient (Letaw, Silberberg, & Tsao 1993, Seo & Ptuskin 1994, Heinbach & Simon 1995, Simon & Heinbach 1996). The spatial diffusion coefficient for the case of reacceleration assumes a Kolmogorov spectrum of weak MHD turbulence so $D_{xx} = \beta D_0 (\rho/\rho_0)^\delta$ with $\delta = 1/3$ for all rigidities. For this case the momentum-space diffusion coefficient D_{pp} is related to the spatial coefficient using the formula given by Seo & Ptuskin (1994), and Berezinskii et al. (1990)

$$D_{pp} D_{xx} = \frac{4 p^2 {v_A}^2}{3\delta(4-\delta^2)(4-\delta) w} \ , \tag{1}$$

where w characterises the level of turbulence, and is equal to the ratio of MHD wave energy density to magnetic field energy density. The free parameter in this relation is v_A^2/w, where v_A is the Alfvén speed; we take $w = 1$ (Seo & Ptuskin 1994).

The adopted distributions of atomic and molecular hydrogen and of ionized hydrogen are described in detail in Paper III; Fig. 1 shows the radial distribution of density in the Galactic plane. The He/H ratio of the interstellar gas is taken as 0.11 by number (see Paper III for a discussion).

The distribution of cosmic-ray sources is chosen to reproduce (after propagation) the cosmic-ray distribution determined by analysis of EGRET γ-ray data (Strong & Mattox 1996). The form used is

$$q(R,z) = q_0 \left(\frac{R}{R_\odot}\right)^\eta e^{-\xi \frac{R-R_\odot}{R_\odot} - \frac{|z|}{0.2\ \mathrm{kpc}}} \ , \tag{2}$$

where q_0 is a normalization constant, η and ξ are parameters; the R-dependence has the same parameterization as that used for SNR by Case & Bhattacharya (1996, 1998). We compute models with their SNR distribution, but also with different parameters to better fit the γ-ray gradient. We apply a cutoff in the source distribution at $R = 20$ kpc since it is unlikely that significant sources are present at such large radii. The z-dependence of q is nominal and reflects simply the assumed confinement of sources to the disk.

The primary propagation is computed first giving the primary distribution as a function of (R, z, p); then the secondary source function is obtained from the gas density and cross sections, and finally the secondary propagation is computed. The bremsstrahlung and inverse Compton γ-rays are computed self-consistently from the gas and radiation fields used for the propagation. The π^0-decay γ-rays are calculated explicitly from the proton and Helium spectra using Dermer's (1986) approach. The secondary nucleon and secondary $e^\pm$ source functions are computed from the propagated primary distribution and the gas distribution.

4. Propagation equation

The propagation equation we use is written in the form:

$$\frac{\partial \psi}{\partial t} = q(\vec{r},p) + \vec{\nabla}\cdot(D_{xx}\vec{\nabla}\psi - \vec{V}\psi) + \frac{\partial}{\partial p}p^2 D_{pp}\frac{\partial}{\partial p}\frac{1}{p^2}\psi - \frac{\partial}{\partial p}\left[\dot{p}\psi - \frac{p}{3}(\vec{\nabla}\cdot\vec{V})\psi\right] - \frac{1}{\tau_f}\psi - \frac{1}{\tau_r}\psi \ , \tag{3}$$

where $\psi = \psi(\vec{r},p,t)$ is the density per unit of total particle momentum, $\psi(p)dp = 4\pi p^2 f(\vec{p})$ in terms of phase-space density $f(\vec{p})$, $q(\vec{r},p)$ is the source term, D_{xx} is the spatial diffusion coefficient, $\vec{V}$ is the convection velocity, reacceleration is described as diffusion in momentum space and is determined by the coefficient D_{pp}, $\dot{p} \equiv dp/dt$ is the momentum loss rate, τ_f is the time scale for fragmentation, and τ_r is the time scale for the radioactive decay.

The numerical solution of the transport equation is based on a Crank-Nicholson (Press et al. 1992) implicit second-order scheme. The three spatial boundary conditions

$$\psi(R_h,z,p) = \psi(R,\pm z_h,p) = 0 \tag{4}$$

are imposed on each iteration.

We use particle momentum as the kinematic variable since it greatly facilitates the inclusion of the diffusive reacceleration terms. The injection spectrum of primary nucleons is assumed to be a power law in momentum for the different species, $dq(p)/dp \propto p^{-\Gamma}$ for the injected *density* as

expected for diffusive shock acceleration (e.g., Blandford & Ostriker 1980). This corresponds to an injected *flux* per kinetic energy interval $dF(E_k)/dE_k \propto p^{-\Gamma}$, a form often used; the value of Γ can vary with species. The injection spectrum for ^{12}C and ^{16}O was taken as $dq(p)/dp \propto p^{-2.35}$, for the case of no reacceleration, and $p^{-2.25}$ with reacceleration. These values are consistent with Engelmann et al. (1990) who give an injection index 2.23 ± 0.05. The same indices reproduce the observed proton and ^{4}He spectra (Paper II). For primary electrons, the injection spectrum can be adjusted to reproduce direct measurements or γ-ray and synchrotron data; all details are given in our series of papers (I–V).

For secondary nucleons, the source term is $q(\vec{r},p) = \beta c\, \psi_p(\vec{r},p)[\sigma_H^{ps}(p) n_H(\vec{r}) + \sigma_{He}^{ps}(p) n_{He}(\vec{r})]$, where $\sigma_H^{ps}(p)$, $\sigma_{He}^{ps}(p)$ are the production cross sections for the secondary from the progenitor on H and He targets, ψ_p is the progenitor density, and n_H, n_{He} are the interstellar hydrogen and Helium number densities.

To compute B/C and ^{10}Be/ ^{9}Be it is sufficient for our purposes to treat only one principal progenitor and compute weighted cross sections based on the observed cosmic-ray abundances, which we took from Lukasiak et al. (1994b). Explicitly, for a principal primary with abundance I_p, we use for the production cross section $\overline{\sigma}^{ps} = \sum_i \sigma^{is} I_i / I_p$, where σ^{is}, I_i are the cross sections and abundances of all species producing the given secondary. For the case of Boron, the Nitrogen progenitor is secondary but only accounts for $\approx 10\%$ of the total Boron production, so that the approximation of weighted cross sections is sufficient.

For the fragmentation cross sections we use the formula given by Letaw, Silberberg, & Tsao (1983). For the secondary production cross sections we use the Webber, Kish, & Schrier (1990) parameterizations in the form of code obtained from the Transport Collaboration (Guzik et al. 1997). For the important B/C ratio, we take the ^{12}C, ^{16}O $\rightarrow$ ^{10}B, ^{10}C, ^{11}B, ^{11}C cross sections from the fit to experimental data given by Heinbach & Simon (1995). For electrons and positrons the same propagation equation is valid when the appropriate energy loss terms (ionization, bremsstrahlung, inverse Compton, synchrotron) are used. The energy loss formulae for these loss mechanisms are given in Paper III.

5. Evaluation of models

We consider the cases of diffusion+convection and diffusion+reacceleration, since these are the minimum combinations which can reproduce the key observations. In principle all three processes could be significant, and such a general model can be considered if independent astrophysical information or models, for example for a Galactic wind (e.g., Zirakashvili et al. 1996, Ptuskin et al. 1997), were to be used.

In our evaluations we use the B/C data summarized by Webber et al. (1996), from HEAO–3 and Voyager 1 and 2. The spectra were modulated to 500 MV appropriate to this data using the force-field approximation (Gleeson & Axford 1968). We also show B/C values from Ulysses

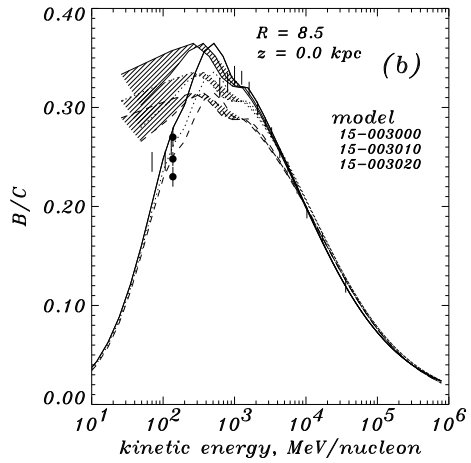

Fig. 2.— B/C ratio for diffusion/convection models without break in diffusion coefficient, for z_h = 3 kpc, dV/dz = 0 (solid line), 5 (dotted line), and 10 km s^{-1} kpc^{-1} (dashed line). Solid line: interstellar ratio, shaded area: modulated to 300–500 MV. Data: vertical bars: HEAO-3, Voyager (Webber et al. 1996), filled circles: Ulysses (DuVernois, Simpson, & Thayer 1996: Φ = 600, 840, 1080 MV).

(DuVernois, Simpson, & Thayer 1996) for comparison, but since this has large modulation (600–1080 MV) we do not base conclusions on these values. We use the measured ^{10}Be/ ^{9}Be ratio from Ulysses (Connell 1998) and from Voyager–1,2, IMP–7/8, ISEE–3 as summarized by Lukasiak et al. (1994a).

The source distribution adopted has $\eta = 0.5$, $\xi = 1.0$ in eq. (2) (apart from the cases with SNR source distribution). This form adequately reproduces the small observed γ-ray based gradient, for all z_h; a more detailed discussion is given in Section 6.

5.1. Diffusion/convection models

The main parameters are z_h, D_0, δ_1, δ_2 and ρ_0 and dV/dz. We treat z_h as the main unknown quantity, and consider values 1–20 kpc. For a given z_h we show B/C for a series of models with different dV/dz.

Fig. 2 shows the case of no break, $\delta_1 = \delta_2$; for each dV/dz, the remaining parameters D_0, δ_1 and ρ_0 are adjusted to fit the data as well as possible. It is clear that a *good* fit is *not* possible; the basic effect of convection is to reduce the variation of B/C with energy, and although this improves the fit at low energies the characteristic peaked shape of the measured B/C cannot be reproduced. Although modulation makes the comparison with the low energy Voyager data somewhat uncertain, Fig. 2 shows that the fit is unsatisfactory; the same is true even if we use a

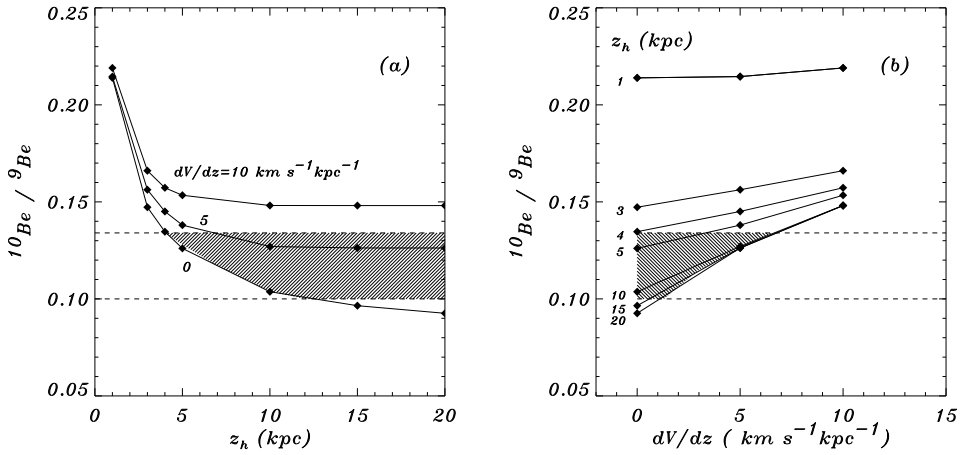

Fig. 3.— Predicted ^{10}Be/ ^{9}Be ratio as function of (a) z_h for dV/dz = 0, 5, 10 km s^{-1} kpc^{-1}, (b) dV/dz for $z_h = 1 - 20$ kpc at 525 MeV/nucleon corresponding to the mean interstellar value for the Ulysses data (Connell 1998); the Ulysses experimental limits are shown as horizontal dashed lines. The shaded regions show the parameter ranges allowed by the data.

very low modulation parameter (300 MV) in an attempt to improve the fit. This modulation is near the minimum value for the entire Voyager 17 year period (cf. the average value of 500 MV; Webber et al. 1996). The failure to obtain a good fit is an important conclusion since it shows that the simple inclusion of convection cannot solve the problem of the low-energy falloff in B/C.

We can however force a fit to the data by allowing a break in $D_{xx}(p)$, i.e. $\delta_1 \neq \delta_2$. In the absence of convection, the falloff in B/C at low energies requires that the diffusion coefficient increases rapidly below $\rho_0 = 3$ GV ($\delta_1 \sim -0.6$) reversing the trend from higher energies ($\delta_2 \sim +0.6$). Inclusion of the convective term does not reduce the size of the *ad hoc* break in the diffusion coefficient, in fact it rather exacerbates the problem by requiring a larger break[1].

Fig. 3 summarizes the limits on z_h and dV/dz, using the ^{10}Be/ ^{9}Be ratio at the interstellar energy of 525 MeV/nucleon appropriate to the Ulysses data (Connell 1998). For $z_h < 4$ kpc, the predicted ratio is always too high, even for no convection; no convection is allowed for such z_h values since this increases ^{10}Be/ ^{9}Be still further. For $z_h \geq 4$ kpc agreement with ^{10}Be/ ^{9}Be is possible provided $0 < dV/dz < 7$ km s^{-1} kpc^{-1}. We conclude from Fig. 3a that in the absence of convection 4 kpc $< z_h <$ 12 kpc, and if convection is allowed the lower limit remains but no upper limit can be set. It is interesting that an upper as well as a lower limit on z_h is obtained in the

[1] Note that the dependence of interaction rate on particle velocity itself is not sufficient to cause the full observed low-energy falloff. In leaky-box treatments the low-energy behaviour is modelled by adopting a constant path-length below a few GeV/nucleon, without attempting to justify this physically. A convective term is often invoked, but our treatment shows that this alone is not sufficient.

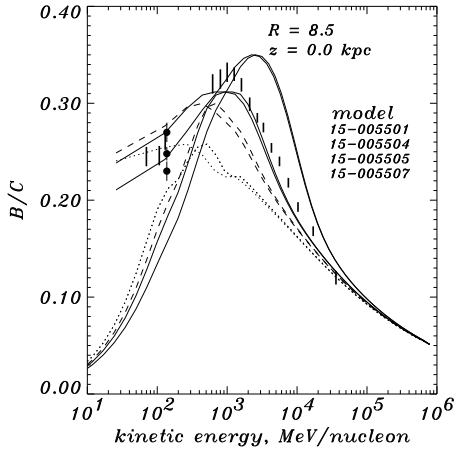

Fig. 4.— B/C ratio for diffusive reacceleration models with $z_h = 5$ kpc, $v_A = 0$ (dotted), 15 (dashed), 20 (thin solid), 30 km s^{-1} (thick solid). In each case the interstellar ratio and the ratio modulated to 500 MV is shown. Data: as Fig. 2.

case of no convection, although ^{10}Be/ ^{9}Be approaches asymptotically a constant value for large halo sizes and becomes insensitive to the halo dimension. From Fig. 3b, $dV/dz < 7$ km s^{-1} kpc^{-1} and this figure places upper limits on the convection parameter for each halo size. These limits are rather strict, and a finite wind velocity is only allowed in any case for $z_h > 4$ kpc. Note that these results are not very sensitive to modulation since the predicted ^{10}Be/ ^{9}Be is fairly constant from 100 to 1000 MeV/nucleon.

5.2. Diffusive reacceleration models

The main parameters are z_h, D_0 and v_A. Again we treat z_h as the main unknown quantity. The evaluation is simpler than for convection models since the number of free parameters is smaller. Fig. 4 illustrates the effect on B/C of varying v_A, from $v_A = 0$ (no reacceleration) to $v_A = 30$ km s^{-1}, for $z_h = 5$ kpc. This shows how the initial form becomes modified to produce the characteristic peaked shape. Reacceleration models thus lead naturally to the observed peaked form of B/C, as pointed out by several previous authors (e.g., Letaw, Silberberg, & Tsao 1993, Seo & Ptuskin 1994, Heinbach & Simon 1995).

Fig. 5 shows ^{10}Be/ ^{9}Be for the same models, (a) as a function of energy for various z_h, (b) as a function of z_h at 525 MeV/nucleon corresponding to the Ulysses measurement. Comparing with the Ulysses data point, we conclude that 4 kpc $< z_h <$ 12 kpc. Again the result is not very sensitive to modulation since the predicted ^{10}Be/ ^{9}Be is fairly constant from 100 to 1000 MeV/nucleon.

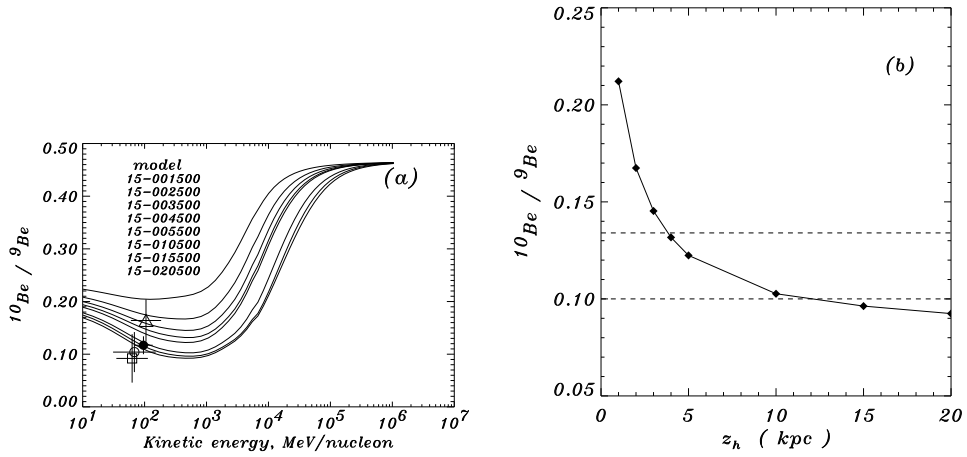

Fig. 5.— ^{10}Be/ ^{9}Be ratio for diffusive reacceleration models: (a) as function of energy for (from top to bottom) z_h = 1, 2, 3, 4, 5, 10, 15 and 20 kpc; (b) as function of z_h at 525 MeV/nucleon corresponding to the mean interstellar value for the Ulysses data (Connell 1998); the Ulysses experimental limits are shown as horizontal dashed lines. Data points from Lukasiak et al. (1994a) (Voyager-1,2: square, IMP-7/8: open circle, ISEE-3: triangle) and Connell (1998) (Ulysses): filled circle.

Energy losses attenuate the flux of stable nuclei much more than radioactive nuclei, and hence lead to an increase in ^{10}Be/ ^{9}Be. Clearly if losses are ignored the predicted ratio will be too low and the derived value of z_h will be too small since z_h will have to be reduced to fit the observations.

Our results on the halo size can be compared with those of other studies: $z_h \geq 7.8$ kpc (Freedman et al. 1980), $z_h \leq 3$ kpc (Bloemen et al. 1993), and $z_h \leq 4$ kpc (Webber, Lee, & Gupta 1992). Lukasiak et al. (1994a) found 1.9 kpc $< z_h <$ 3.6 kpc (for no convection) based on Voyager Be data and using the Webber, Lee, & Gupta (1992) models. We believe our new limits to be an improvement, first because of the improved Be data from Ulysses, second because of our treatment of energy losses (see Section 5.2) and generally more realistic astrophysical details in our model. Recently, Webber & Soutoul (1998), Ptuskin & Soutoul (1998) have obtained $z_h = 2 - 4$ kpc and 4.9^{+4}_{-2} kpc, respectively, in agreement with our results.

6. Cosmic-ray gradients

An important constraint on any model of cosmic-ray propagation is provided by γ-ray data which give information on the radial distribution of cosmic rays in the Galaxy. For a given source distribution, a large halo will give a smaller cosmic-ray gradient. It is generally believed that supernova remnants (SNR) are the main sources of cosmic rays (see Webber 1997 for a recent

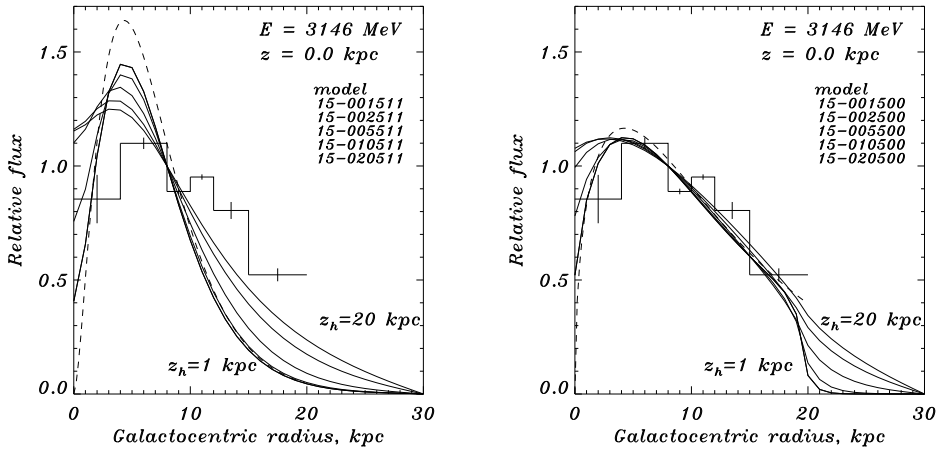

Fig. 6.— *Left panel*: Radial distribution of 3 GeV protons at $z = 0$, for diffusive reacceleration model with halo sizes $z_h = 1$, 3, 5, 10, 15, and 20 kpc (solid curves). The source distribution is that for SNR given by Case & Bhattacharya (1996), shown as a dashed line. The cosmic-ray distribution deduced from EGRET >100 MeV γ-rays (Strong & Mattox 1996) is shown as the histogram. *Right panel*: Radial distribution of 3 GeV protons at $z = 0$, for diffusive reacceleration model with various halo sizes $z_h = 1$, 3, 5, 10, 15, and 20 kpc (solid curves). The source distribution used is shown as a dashed line. It was adopted to reproduce the cosmic-ray distribution deduced from EGRET >100 MeV γ-rays (Strong & Mattox 1996) which is shown as the histogram.

review), but unfortunately the distribution of SNR is poorly known due to selection effects. Nevertheless it is interesting to compare quantitatively the effects of halo size on the gradient for a plausible SNR source distribution. For illustration we use the SNR distribution from Case & Bhattacharya (1996), which is peaked at $R = 4 - 5$ kpc and has a steep falloff towards larger R.

Fig. 6 (left panel) shows the effect of halo size on the resulting radial distribution of 3 GeV cosmic-ray protons, for the reacceleration model. For comparison we show the cosmic-ray distribution deduced by model-fitting to EGRET γ-ray data (> 100 MeV) from Strong & Mattox (1996), which is dominated by the π^0-decay component generated by GeV nucleons; the analysis by Hunter et al. (1997), based on a different approach, gives a similar result. The predicted cosmic-ray distribution using the SNR source function is too steep even for large halo sizes; in fact the halo size has a relatively small effect on the distribution. Other related distributions such as pulsars (Taylor, Manchester & Lyne 1993, Johnston 1994) have an even steeper falloff. Only for $z_h = 20$ kpc does the gradient approach that observed, and in this case the combination of a large halo and a slightly less steep SNR distribution could give a satisfactory fit. For diffusion/convection models the situation is similar, with more convection tending to make the gradient follow more closely the sources. A larger halo ($z_h \gg 20$ kpc), apart from being excluded by the ^{10}Be analysis presented here, would in fact not improve the situation much since Fig. 6

shows that the gradient approaches an asymptotic shape which hardly changes beyond a certain halo size. This is a consequence of the nature of the diffusive process, which even for an unlimited propagation region still retains the signature of the source distribution.

Based on these results we have to conclude, in the context of the present models, that the distribution of sources is not that expected from the (highly uncertain: see Green 1991) distribution of SNR. This conclusion is similar to that previously found by others (Webber, Lee, & Gupta 1992, Bloemen et al. 1993). In view of the difficulty of deriving the SNR distribution this is perhaps not a serious shortcoming; if SNR are indeed cosmic-ray sources then it is possible that the γ-ray analysis gives the best estimate of their Galactic distribution. Therefore in our standard model we have obtained the source distribution empirically by requiring consistency with the high energy γ-ray results.

Alternatively it is possible that the diffusion is not isotropic but occurs preferentially in the radial direction, so smoothing the source distribution more effectively. This possibility will be addressed in future work.

Fig. 6 (right panel) shows the source distribution adopted in the present work, and the resulting 3 GeV proton distribution, again compared to that deduced from γ-rays. The gradients are now consistent, especially considering that some systematic effects, due for example unresolved γ-ray sources, are present in the γ-ray based distribution.

7. Interstellar positrons and antiproton spectra

The positron and antiproton fluxes reflect the proton and Helium spectra throughout the Galaxy and thus provide an essential check on propagation models and also on the interpretation of diffuse γ-ray emission (Paper IV). Secondary positrons and antiprotrons in Galactic cosmic rays are produced in collisions of cosmic-ray particles with interstellar matter[2]. These are an important diagnostic for models of cosmic-ray propagation and provide information complementary to that provided by secondary nuclei. However, unlike secondary nuclei, antiprotons reflect primarily the propagation history of the protons, the main cosmic-ray component.

In our model the proton and Helium spectra are computed as a function of (R, z, p) by the propagation code. The injection spectrum is adjusted to give a good fit to the locally measured spectrum, normalizing at 10 GeV/nucleon.

For the injection spectra of protons, we find $\Gamma = 2.15$ reproduces the observed spectra in the case of no reacceleration, and $\Gamma = 2.25$ with reacceleration. We find it is necessary to use slightly steeper (0.2 in the index) injection spectra for Helium nuclei in order to fit the observed spectra

[2] Secondary origin of cosmic-ray antiprotons is basically accepted, though some other exotic contributors such as, e.g., neutralino annihilation (Bottino et al. 1998) are also discussed.

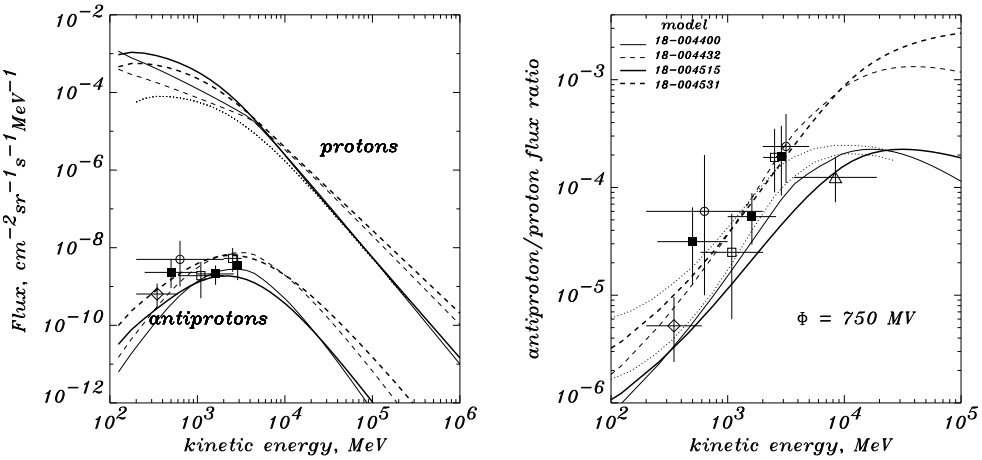

Fig. 7.— *Left panel:* Interstellar nucleon and antiproton spectra as calculated in nonreacceleration models (thin lines) and models with reacceleration (thick lines). Proton spectra consistent with the local one are shown by the solid lines, hard spectra are shown by the dashed lines. The local spectrum as measured by IMAX (Menn et al. 1997) is shown by dots. *Right panel:* $\bar{p}/p$ ratio for different ambient proton spectra. Lines are coded as on the left. The ratio is modulated with $\Phi = 750$ MV. Calculations of Simon et al. (1998) are shown by the dotted lines. Data: see references in Paper IV.

in the 1–100 GeV range of interest for positron production. The spectra fit up to about 100 GeV beyond which the Helium spectrum without reacceleration becomes too steep and the proton spectrum with reacceleration too flat; these deviations are of no consequence for the positron and antiproton calculations.

Our calculations of the interstellar antiproton spectra and $\bar{p}/p$ ratio for these spectra are shown in Fig. 7. The computed antiproton spectrum is divided by the same interstellar proton spectrum, and the ratio is modulated to 750 MV. The corresponding ratios are shown on the right panel. We have performed the same calculations for models with and without reacceleration and the results differ only in details. As seen, our result agrees well with the calculations of Simon et al. (1998), showing that our treatment of the production cross-sections is adequate (for the details of the cross sections see Paper IV).

Fig. 8 shows the computed secondary positron spectra for the cases without and with reacceleration. Our predictions are compared with recent absolute measurements above a few GeV where solar modulation is small (Barwick et al. 1998), and the agreement is satisfactory in both cases; this comparison has the advantage of being independent of the electron spectrum, unlike the positron/electron ratio which was the main focus of Paper II.

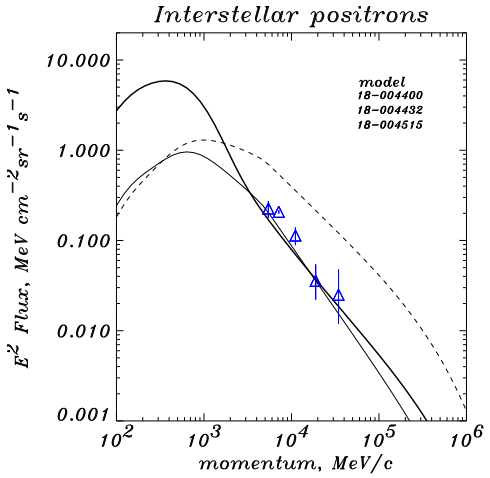

Fig. 8.— Spectra of secondary positrons for 'conventional' (thin line) and hard (dashes) nucleon spectra (no reacceleration). Thick line: 'conventional' case with reacceleration. Data: Barwick et al. (1998).

8. Probes of the interstellar nucleon spectrum

Diffuse Galactic γ-ray observations have been interpreted as requiring a harder average nucleon spectrum in interstellar space than that observed directly (Hunter et al. 1997, Gralewicz et al. 1997, Mori 1997, Moskalenko & Strong 1998b,c, see also Section 9). A sensitive test of the interstellar nucleon spectra is provided by secondary antiprotons and positrons. Because they are secondary, they reflect the *large-scale* nucleon spectrum independent of local irregularities in the primaries.

We consider a case which matches the γ-ray data (Fig. 9) at the cost of a much harder proton spectrum than observed. The dashed lines in Fig. 7 (right) show the $\bar{p}/p$ ratio for the hard proton spectrum (with and without reacceleration); the ratio is still consistent with the data at low energies but rapidly increases toward higher energies and becomes $\sim$4 times higher at 10 GeV. Up to 3 GeV it does not confict with the data with their very large error bars. It is however larger than the point at 3.7–19 GeV (Hof et al. 1996) by about 5σ. Clearly we cannot conclude definitively on the basis of this one point[3], but it does indicate the sensitivity of this test. In view of the sharply rising ratio in the hard-spectrum scenario it seems unlikely that the data could be fitted in this case even with some re-scaling due to propagation uncertainties. More experiments are planned (see Paper IV for a summary) and these should allow us to set stricter limits on the nucleon spectra including less extreme cases than considered here, and to constrain better the

[3] We do not consider here the older $\bar{p}$ measurement of Golden et al. (1984a) because the flight of the early instrument in 1979 was repeated in 1991 with significantly improved instrument and analysis techniques (see Hof et al. 1996 and a discussion therein).

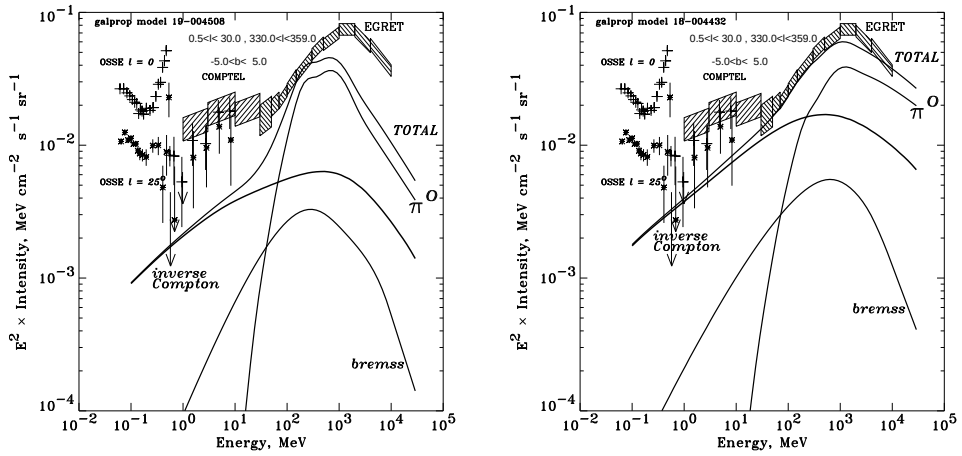

Fig. 9.— Gamma-ray energy spectrum of the inner Galaxy ($300° \leq l \leq 30°$, $|b| \leq 5°$) compared with our model calculations. Data: EGRET (Strong & Mattox 1996), COMPTEL (Strong et al. 1998), OSSE ($l = 0, 25°$: Kinzer, Purcell, & Kurfess 1997). *Left panel:* Model with 'conventional' nucleon and electron spectra. Also shown are the contributions of individual components: bremsstrahlung, inverse Compton, and π^0-decay. *Right panel:* The same compared to the model with the *hard nucleon* spectrum (no reacceleration).

interpretation of γ-rays.

Positrons also provide a good probe of the nucleon spectrum, but are more affected by energy losses and propagation uncertainties. Fig. 8 shows, in addition to the normal case, the positron flux resulting from a hard nucleon spectrum. The predicted flux is a factor 4 above the Barwick et al. (1998) measurements and hence provides further evidence against the 'hard nucleon spectrum' hypothesis.

9. Diffuse Galactic continuum gamma rays

We can also use our model to study the diffuse γ-ray emission from the Galaxy. Recent results from both COMPTEL and EGRET indicate that inverse Compton (IC) scattering is a more important contributor to the diffuse emission that previously believed. COMPTEL results (Strong et al. 1997) for the 1–30 MeV range show a latitude distribution in the inner Galaxy which is broader than that of HI and H_2, so that bremsstrahlung of electrons on the gas does not appear adequate and a more extended component such as IC is required. The broad distribution is the

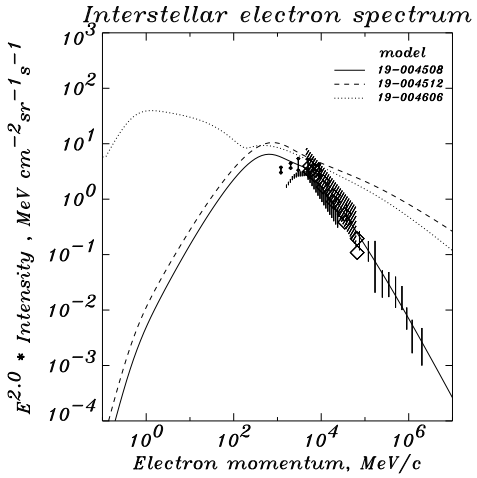

Fig. 10.— Electron spectra at $R_\odot = 8.5$ kpc in the plane, for 'conventional' (solid line), and hard electron spectrum models without (dashes), and with (dots) low-energy upturn. Data (direct measurements): Taira et al. (1993) (vertical lines), Golden et al. (1984b, 1994) (shaded areas), Ferrando et al. (1996) (small diamonds), Barwick et al. (1998) (large diamonds).

result of the large z-extent of the interstellar radiation field[4] which can interact with cosmic-ray electrons up to several kpc from the plane. At much higher energies, the puzzling excess in the EGRET data above 1 GeV relative to that expected for π^0-decay has been suggested to orginate in IC scattering from a hard interstellar electron spectrum (e.g., Pohl & Esposito 1998).

Fig. 9 (left) shows the γ-ray spectrum of the inner Galaxy for a 'conventional' case which matches the directly measured electron and nucleon spectra and is consistent with synchrotron spectral index data (Moskalenko & Strong 1998c, Paper V). Fig. 10 shows electron spectra at $R_\odot = 8.5$ kpc in the disk for this model. It fits the observed γ-ray spectrum only in the range 30 MeV – 1 GeV. Fig. 9 (right) shows the case of π^0-decay γ-rays from a hard nucleon spectrum (but still the 'conventional' electron spectrum). This can improve the fit above 1 GeV but the high energy antiproton and positron data probably exclude the hypothesis that the local nucleon spectrum differs significantly from the Galactic average (see Section 8).

We thus consider the 'hard electron spectrum' alternative. The electron injection spectral index is taken as –1.7 (with reacceleration), which after propagation provides consistency with radio synchrotron data (a crucial constraint). Following Pohl & Esposito (1998), for this model we do *not* require consistency with the locally measured electron spectrum above 10 GeV since the rapid energy losses cause a clumpy distribution so that this is not necessarily representative of the interstellar average. For this case, the interstellar electron spectrum deviates strongly from

[4] We have made a new calculation of the interstellar radiation field (Paper V) based on stellar population models and IRAS and COBE data.

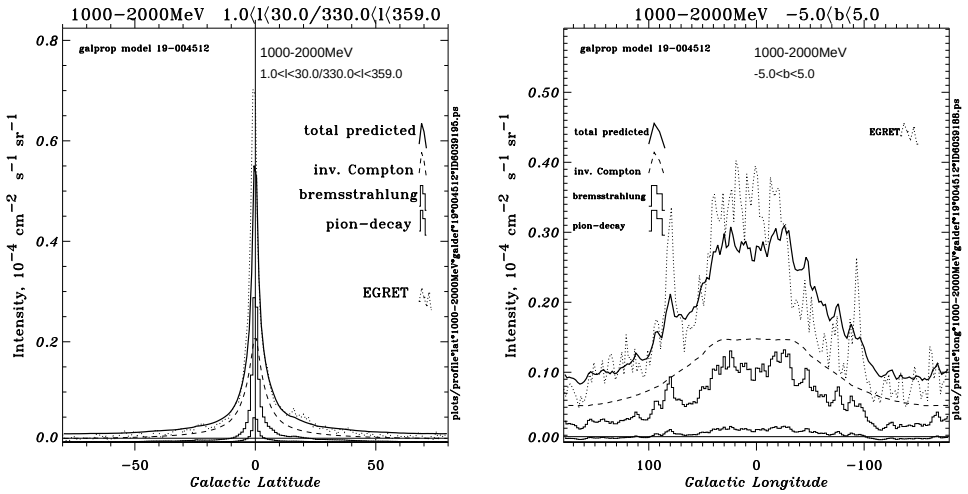

Fig. 11.— Distributions of 1–2 GeV γ-rays computed for a hard electron spectrum (reacceleration model) as compared to EGRET data (Cycles 1–4, point sources removed, see Paper V). Contribution of various components is shown as calculated in our model. *Left panel:* Latitude distribution ($330^\circ < l < 30^\circ$). *Right panel:* Longitude distribution for $|b| < 5^\circ$.

that locally measured as illustrated in Fig. 10. Because of the increased IC contribution at high energies, the predicted γ-ray spectrum can reproduce the overall intensity from 30 MeV – 10 GeV but the detailed shape above 1 GeV is still problematic. Further refinement of this scenario is presented in Paper V.

Fig. 11 shows the model latitude and longitude γ-ray distributions for the inner Galaxy for 1–2 GeV, convolved with the EGRET point-spread function, compared to EGRET Phase 1–4 data (with known point sources subtracted). It shows that a model with large IC component can indeed reproduce the data. The latitude distribution here is not as wide as at low energies owing to the rapid energy losses of the electrons, so that an observational distinction between a gas-related π^0-component from a hard nucleon spectrum and the IC model does not seem possible on the basis of γ-rays alone, but requires also other tests such as consistency with antiproton and positron data (see Section 8).

None of these models fits the γ-ray spectrum below $\sim$30 MeV as measured by the Compton Gamma-Ray Observatory (Fig. 12 left). In order to fit the low-energy part as diffuse emission (Fig. 12 right), without violating synchrotron constraints (Paper V), requires a rapid upturn in the cosmic-ray electron spectrum below 200 MeV (e.g., as in Fig. 10). However, in view of the energetics problems (Skibo et al. 1997), a population of unresolved sources seems more probable and would be the natural extension of the low energy plane emission seen by OSSE (Kinzer, Purcell, & Kurfess 1997) and GINGA (Yamasaki et al. 1997).

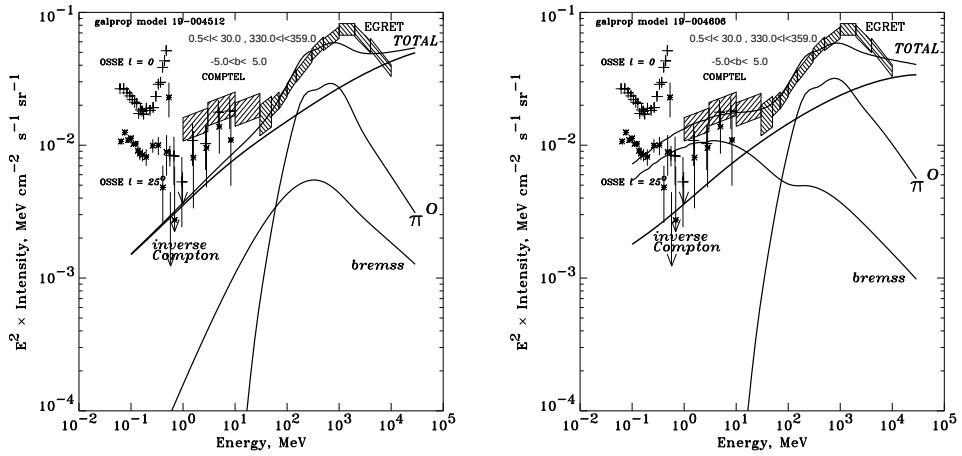

Fig. 12.— γ-ray spectrum of inner Galaxy compared to models with a hard electron spectrum without (left) and with low-energy upturn (right). Data as in Fig. 9.

10. Conclusions

Our propagation model has been used to study several areas of high energy astrophysics. We believe that combining information from classical cosmic-ray studies with γ-ray and other data leads to tighter constraints on cosmic-ray origin and propagation.

We have shown that simple diffusion/convection models have difficulty in accounting for the observed form of the B/C ratio without special assumptions chosen to fit the data, and do not obviate the need for an *ad hoc* form for the diffusion coefficient. On the other hand we confirm the conclusion of other authors that models with reacceleration account naturally for the energy dependence over the whole observed range. Combining these results points rather strongly in favour of the reacceleration picture.

We take advantage of the recent Ulysses Be measurements to obtain estimates of the halo size. Our limits on the halo height are 4 kpc $< z_h <$ 12 kpc. Our new limits should be an improvement on previous estimates because of the more accurate Be data, our treatment of energy losses, and the inclusion of more realistic astrophysical details (such as, e.g., the gas distribution) in our model. The gradient of protons derived from γ-rays is smaller than expected for SNR sources, and we therefore adopt a flatter source distribution in order to meet the γ-ray constraints. This may just reflect the uncertainty in the SNR distribution.

The positron and antiproton fluxes calculated are consistent with the most recent measurements. The $\bar{p}/p$ data point above 3 GeV and positron flux measurements seem to rule out the hypothesis that the local cosmic-ray nucleon spectrum differs significantly from the Galactic average (by implication adding support to the 'hard electron' alternative), but confirmation of this conclusion must await more accurate antiproton data at high energies.

Gamma-ray data suggest that the interstellar electron spectrum is harder then that locally measured, but this remains to be confirmed by detailed study of the angular distribution. The low-energy Galactic γ-ray emission is difficult to explain as truly diffuse and a point source population seems more probable.

REFERENCES

Barwick, S. W., et al. 1998, ApJ, 498, 779

Berezinskii, V. S., et al. 1990, Astrophysics of Cosmic Rays (Amsterdam: North Holland)

Blandford, R. D., & Ostriker, J. P. 1980, ApJ, 237, 793

Bloemen, H., Dogiel, V. A., Dorman, V. I., & Ptuskin, V. S. 1993, A&A, 267, 372

Bottino, A., Donato, F., Formengo, N., & Salati, P. 1998, Phys. Rev. D, 58, 123503

Case, G., & Bhattacharya, D. 1996, A&AS, 120C, 437

Case, G., & Bhattacharya, D. 1998, ApJ, 504, 761

Connell, J. J. 1998, ApJ, 501, L59

Dermer, C. D. 1986, A&A, 157, 223

DuVernois, M. A., Simpson, J. A., & Thayer, M. R. 1996, A&A, 316, 555

Engelmann, J. J., et al. 1990, A&A, 233, 96

Ferrando, P., et al. 1996, A&A, 316, 528

Freedman, I., Kearsey, S., Osborne, J. L., & Giler, M. 1980, A&A, 82, 110

Ginzburg, V. L., Khazan, Ya. M., & Ptuskin, V. S. 1980, Ap&SS, 68, 295

Gleeson, L. J., & Axford, W. I. 1968, ApJ, 154, 1011

Golden, R. L., et al. 1984a, Astrophys. Lett., 24, 75

Golden, R. L., et al. 1984b, ApJ, 287, 622

Golden, R. L., et al. 1994, ApJ, 436, 769

Gralewicz, P., et al. 1997, A&A, 318, 925

Green, D. A. 1991, PASP, 103, 209

Guzik, T. G., et al. 1997, in Proc. 25th Int. Cosmic Ray Conference (Durban), 4, 317

Heinbach, U., & Simon, M. 1995, ApJ, 441, 209

Hof, M., et al. 1996, ApJ, 467, L33

Hunter, S. D., et al. 1997, ApJ, 481, 205

Johnston, S. 1994, MNRAS, 268, 595

Jokipii, J. R. 1976, ApJ, 208, 900

Jones, F. C. 1979, ApJ, 229, 747

Kinzer, R. L., Purcell, W. R., & Kurfess, J. D. 1997, in AIP Conf. Proc. 410, Fourth Compton Symposium, ed. C. D. Dermer, M. S. Strickman, & J. D. Kurfess (New York: AIP), p.1193 (OSSE preprint #89)

Lerche, I., & Schlickeiser, R. 1982, A&A, 107, 148

Letaw, J. R., Silberberg, R., & Tsao, C. H. 1983, ApJS, 51, 271

Letaw, J. R., Silberberg, R., & Tsao, C. H. 1993, ApJ, 414, 601

Lukasiak, A., Ferrando, P., McDonald, F. B., & Webber, W. R. 1994a, ApJ, 423, 426

Lukasiak, A., Ferrando, P., McDonald, F. B., & Webber, W. R. 1994b, ApJ, 426, 366

Menn, W., et al. 1997, in Proc. 25th Int. Cosmic Ray Conference (Durban), 3, 409

Mori, M. 1997, ApJ, 478, 225

Moskalenko, I. V., & Strong, A. W. 1998a, ApJ, 493, 694 (Paper II)

Moskalenko, I. V., & Strong, A. W. 1998b, in Proc. 16th European Cosmic Ray Symp. (Alcala), GR-1.3, in press (astro-ph/9807288)

Moskalenko, I. V., & Strong, A. W. 1998c, in Proc. 3rd INTEGRAL Workshop "The Extreme Universe", paper #36, in press

Moskalenko, I. V., & Strong, A. W. 1998d, ApJ, submitted

Moskalenko, I. V., Strong, A. W., & Reimer, O. 1998, A&A, 338, L75 (Paper IV)

Press, W. H., et al. 1992, Numerical Recipes in FORTRAN, 2nd Edition (Cambridge: Cambridge University Press)

Pohl, M., & Esposito, J. A. 1998, ApJ, 507, 327

Porter, T. A., & Protheroe R. J. 1997, J. Phys. G.: Nucl. Part. Phys., 23, 1765

Ptuskin, V. S., & Soutoul, A. 1998, A&A, 337, 859

Ptuskin, V. S., Völk, H. J., Zirakashvili, V. N., & Breitschwerdt, D. 1997, A&A, 321, 434

Seo, E. S., & Ptuskin, V. S. 1994, ApJ, 431, 705

Simon, M., & Heinbach, U. 1996, ApJ, 456, 519

Simon, M., Molnar, A., & Roesler, S. 1998, ApJ, 499, 250

Simpson, J. A., & Garcia-Munoz, M. 1988, Spa. Sci. Rev., 46, 205

Skibo, J. G., et al. 1997, ApJ, 483, L95

Strong, A. W., & Mattox, J. R. 1996, A&A, 308, L21

Strong, A. W., & Moskalenko, I. V. 1997, in AIP Conf. Proc. 410, Fourth Compton Symposium, ed. C. D. Dermer, M. S. Strickman, & J. D. Kurfess (New York: AIP), p.1162 (Paper I)

Strong, A. W., & Moskalenko, I. V. 1998, ApJ, 509, 212 (Paper III)

Strong, A. W., Moskalenko, I. V., & Reimer, O. 1998, ApJ, submitted (Paper V)

Strong, A. W., et al. 1997, in AIP Conf. Proc. 410, Fourth Compton Symposium, ed. C. D. Dermer, M. S. Strickman, & J. D. Kurfess (New York: AIP), p.1198

Strong, A. W., et al. 1998, in Proc. 3rd INTEGRAL Workshop 'The Extreme Universe', paper #15, in press

Taira, T., et al. 1993, in Proc. 23rd Int. Cosmic Ray Conference (Calgary), 2, 128

Taylor, J. H., Manchester, R. N., & Lyne, A. G. 1993, ApJS, 88, 529

Webber, W. R. 1997, Spa. Sci. Rev., 81, 107

Webber, W. R., & Soutoul, A. 1998, ApJ, 506, 335

Webber, W. R., Kish, J. C., & Schrier, D. A. 1990, Phys. Rev. C, 41, 566

Webber, W. R., Lee, M. A., & Gupta, M. 1992, ApJ, 390, 96

Webber, W. R., Lukasiak, A., McDonald, F. B., & Ferrando, P. 1996, ApJ, 457, 435

Yamasaki, N.Y., et al. 1997, ApJ, 481, 821

Zirakashvili, V. N., Breitschwerdt, D., Ptuskin, V. S., & Völk, H. J. 1996, A&A, 311, 113